Bias in Error-Corrected Quantum Sensing

Ivan Rojkov,[1,*] David Layden,[2,†] Paola Cappellaro,[2] Jonathan Home,[1] and Florentin Reiter[1,‡]
[1]Institute for Quantum Electronics, ETH Zürich, 8093 Zürich, Switzerland
[2]Research Laboratory of Electronics and Department of Nuclear Science and Engineering, Massachusetts Institute of Technology, Cambridge, Massachusetts 02139, USA

(Received 22 January 2021; revised 21 December 2021; accepted 28 January 2022; published 6 April 2022)

The sensitivity afforded by quantum sensors is limited by decoherence. Quantum error correction (QEC) can enhance sensitivity by suppressing decoherence, but it has a side effect: it biases a sensor's output in realistic settings. If unaccounted for, this bias can systematically reduce a sensor's performance in experiment, and also give misleading values for the minimum detectable signal in theory. We analyze this effect in the experimentally motivated setting of continuous-time QEC, showing both how one can remedy it, and how incorrect results can arise when one does not.

DOI: 10.1103/PhysRevLett.128.140503

Introduction.—Quantum sensors use quantum systems and effects to sense an external signal $V(t)$ in their environment, such as electromagnetic fields, temperature or pressure [1]. They also, however, experience decoherence due to this same environment, which limits their sensitivity in practice. Techniques to suppress decoherence, without equally suppressing the signal, are therefore of central importance in quantum sensing [2–9]. Quantum error correction (QEC) is currently emerging as an important technique to this end, and has attracted substantial theoretical and experimental interest of late [10–27]. Indeed, while QEC was first developed in the context of quantum computing, the substantially less demanding experimental requirements of quantum sensing make the latter application particularly attractive for QEC in the near term [28]. It is therefore essential to address the unique challenges that arise from using QEC for sensing, which often lack close analogs in quantum computing (or quantum communication).

Quantum sensing generally works by preparing a sensor in a known initial state, letting it evolve under dynamics that depend on the signal $V(t)$, and then measuring the sensor's final state so as to estimate the signal. In error-corrected quantum sensing, the initial state is a logical state of a QEC code, and errors are repeatedly corrected while the signal imprints on the sensor, until the latter is finally read out. The error correction can either be performed at discrete times through measurement and feedback, or continuously by engineering appropriate dissipative terms in the sensor's dynamics. Most analyses of QEC for sensing to date have focused on the leading-order effective dynamics under very frequent or strong error correction (in the discrete or continuous pictures, respectively) to show that QEC can—in principle—completely suppress decoherence in a sensor.

In this Letter we instead examine quantum sensing under QEC of manifestly finite frequency or strength. As expected, we find that such QEC reduces, but does not fully eliminate decoherence in a sensor. Crucially, however, we also find that it can systematically bias a sensor's output, i.e., introduce inaccuracy that is not reduced by averaging over many runs. Using elementary assumptions, we determine under which condition this bias arises and illustrate it with a canonical example of error-corrected quantum sensing. Fundamentally, it appears from a nonzero delay between an error and its subsequent correction, during which time a sensor typically evolves differently than if no error had occurred. This effect would clearly reduce a sensor's performance in experiment if one failed to account for it. Similarly, we use biased estimator theory to show that a standard analysis can give misleading values of sensitivity in theory. Finally, we give a simple method to remedy both issues through postprocessing of measurement data.

Setting.—We consider the problem of estimating a dc signal $V(t) = V$ using a quantum sensor comprising n identical qubits with a Hamiltonian

$$H = \sum_{j=1}^{n} \left(\frac{\omega_q}{2} \sigma_z^{(j)} + \xi V \sigma_z^{(j)} \right) = \sum_{j=1}^{n} \frac{\omega}{2} \sigma_z^{(j)}, \qquad (1)$$

where ω_q is the qubits' zero-field splitting and ξ is their coupling strength to the environment ($\hbar = 1$). We define for convenience the combined energy gap $\omega := \omega_q + 2\xi V$. We also suppose that the sensor undergoes decoherence described by a Lindblad equation. Following Refs. [10,12,13,17,20], we assume this decoherence to be primarily due to bit flips affecting each qubit independently at the same rate Γ_{err}, described by the Lindblad jump operators $L_{\mathrm{err}}^{(j)} = \sqrt{\Gamma_{\mathrm{err}}} \sigma_x^{(j)}$ [29]. Note that this is a pessimistic model in the sense that dynamical decoupling, one of the main techniques for suppressing decoherence in quantum sensors, is

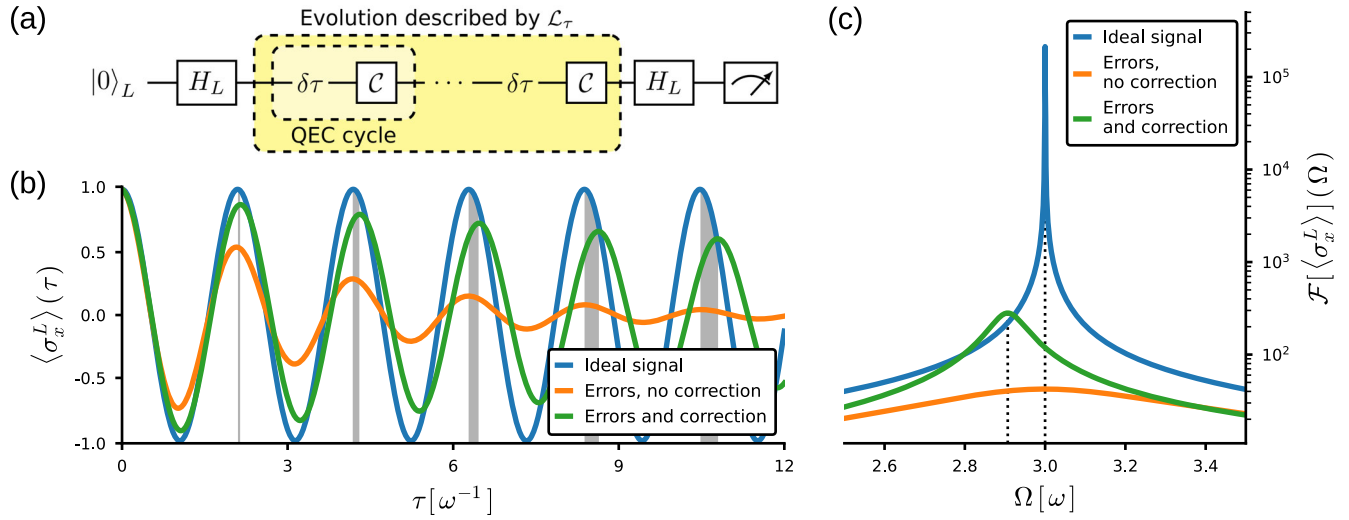

FIG. 1. Bias in error-corrected quantum sensing. (a) Error-corrected Ramsey sequence represented as a quantum circuit where H_L are logical Hadamard gates, $\mathcal{C}$ represents detection and correction processes and $\delta\tau$ free evolution intervals under the signal with frequency ω. The overall dynamics during the sensing time τ is described by $\mathcal{L}_\tau$. In (b), we plot the expectation value $\langle\sigma_x^L\rangle$ as a function of the free evolution time τ for three different sensing models: ideal, uncorrected and error corrected. The parameters used for the simulation are $\Gamma_{\rm err} = 0.1\omega$, $\Gamma_{\rm qec} = 5\omega$. Panel (c) shows the Fourier transform $\mathcal{F}$ of the functions from Fig. 1(b).

largely incompatible with both dc signals and Lindbladian decoherence [1].

This decoherence limits the sensor's achievable sensitivity. It can be suppressed, and the sensitivity enhanced, by using the bit-flip code where $|0\rangle_L = |0\ldots0\rangle$ and $|1\rangle_L = |1\ldots1\rangle$ for $n \geq 3$ qubits. The idea is to mimic a Ramsey interferometry protocol [30] at the logical level. One first prepares a state $(1/\sqrt{2})(|0\rangle_L + |1\rangle_L)$ (say by applying a logical Hadamard, H_L, to $|0\rangle_L$), then lets the sensor evolve for a time τ all the while detecting and correcting $L_{\rm err}^{(j)}$ errors. One then applies H_L to the time-evolved state and measures in the $\{|0\rangle_L, |1\rangle_L\}$ basis, effectively measuring $\sigma_x^L = |0\rangle\langle 1|_L + |1\rangle\langle 0|_L$.

Broadly speaking, errors can be detected and corrected in two ways, both illustrated in Fig. 1(a). One is to periodically measure the parity between qubits at intervals $\delta\tau$ to infer whether an error has occurred, and then to apply appropriate feedback. The other is to engineer additional jump operators in the sensor's Liouvillian $\mathcal{L}_\tau$ that implement a continuous analog of the former scheme. We focus here on the latter, continuous type for mathematical convenience. For $n = 3$, the QEC jump operators have the form [17]

$$L_{\rm qec}^{(j)} = \sqrt{\Gamma_{\rm qec}}\sigma_x^{(j)}\frac{1-\sigma_z^{(j)}\sigma_z^{(k)}}{2}\frac{1-\sigma_z^{(j)}\sigma_z^{(l)}}{2} \tag{2}$$

for $\{j,k,l\} = \{1,2,3\}$. Notice that $L_{\rm qec}^{(j)}$ flips qubit j at a rate $\Gamma_{\rm qec}$ if and only if it disagrees with the other two qubits. The sensor's overall dynamics is then given by the Lindblad equation $\dot{\rho} = \mathcal{L}_\tau(\rho)$ with the Liouvillian

$$\mathcal{L}_\tau(\rho) = -i[H,\rho] + \sum_j \mathcal{D}[L_{\rm err}^{(j)}](\rho) + \sum_j \mathcal{D}[L_{\rm qec}^{(j)}](\rho),$$

where

$$\mathcal{D}[L_k^{(j)}](\rho) \coloneqq L_k^{(j)}\rho L_k^{(j)\dagger} - \frac{1}{2}\left(L_k^{(j)\dagger}L_k^{(j)}\rho + \rho L_k^{(j)\dagger}L_k^{(j)}\right) \tag{3}$$

for a jump operator $L_k^{(j)}$. The bias we are concerned with arises from both types of QEC, with $\Gamma_{\rm qec}$ and $\delta\tau^{-1}$ playing the same role.

Imperfect error-corrected sensing.—Repeating the protocol in Fig. 1(a) gives a set of binary measurement results $\{X_\tau\}$, where $X_\tau = \pm 1$ for $|0\rangle_L/|1\rangle_L$ outcomes, respectively. One can then infer ω with the least-squares estimator

$$\hat{\omega} = \arg\min_\omega \sum_\tau [X_\tau - \langle\sigma_x^L(\tau,\omega,\Gamma_{\rm err},\Gamma_{\rm qec})\rangle]^2, \tag{4}$$

which minimizes the discrepancy between the observed and expected results. For a single, noiseless qubit $\langle\sigma_x\rangle = \cos(\omega\tau)$. Similarly, the three-qubit repetition code gives $\langle\sigma_x^L\rangle = \cos(3\omega\tau)$ in the limit of infinitely frequent or strong QEC ($\Gamma_{\rm qec}$ or $\delta\tau^{-1} \to \infty$)—producing, in effect, a noiseless qubit with a stronger dependence on ω at the logical level. With finite frequency or strength QEC, the logical qubit will gradually decohere, albeit hopefully more slowly than the physical qubits. One might expect that in this latter, realistic setting, $\langle\sigma_x^L\rangle$ would behave like in the ideal case, but with an additional exponential decay that vanishes as $\Gamma_{\rm err} \to 0$:

$$\langle \sigma_x^L \rangle \stackrel{?}{=} e^{-3\Gamma_{\rm err}\tau}\cos(3\omega\tau). \tag{5}$$

We will show, however, that while the true expression for $\langle \sigma_x^L \rangle$ indeed has this form, the coefficients must be replaced by distinct, effective ones $\Gamma_{\rm err} \to \Gamma_{\rm eff}$ and $\omega \to \omega_{\rm eff}$ given by Eq. (9).

Finding $\langle \sigma_x^L \rangle$ amounts to solving a system of first order differential equations describing evolution under $\mathcal{L}_\tau$. We sketch the process here, relegating the details to the Supplemental Material [31]. To get a tractable system, we make the approximation that rare, weight-2 errors cause the state to vanish. This quickly leads to the solution $\langle \sigma_x^L \rangle = 2\mathrm{Re}(q)$, where

$$\begin{aligned} q(\tau) = {} & C_+ e^{\frac{1}{2}\tau(-\Gamma_{\rm qec}-6\Gamma_{\rm err}-4i\omega+\sqrt{D})}, \\ & - C_- e^{\frac{1}{2}\tau(-\Gamma_{\rm qec}-6\Gamma_{\rm err}-4i\omega-\sqrt{D})}. \end{aligned} \tag{6}$$

Here $C_\pm$ are normalization constants (discussed below and in Ref. [31]) and $D = \Gamma_{\rm qec}^2 + 12\,\Gamma_{\rm qec}\Gamma_{\rm err} + 12\,\Gamma_{\rm err}^2 - 4i\,\Gamma_{\rm qec}\,\omega - 4\,\omega^2$ is a discriminant. Expanding this expression for a large—but finite—QEC rate then gives

$$\begin{aligned} \langle \sigma_x^L \rangle = {} & 2C_+ e^{-6\frac{\Gamma_{\rm err}}{\Gamma_{\rm qec}}\Gamma_{\rm err}\tau}\cos\left[3\omega\left(1-2\frac{\Gamma_{\rm err}}{\Gamma_{\rm qec}}\right)\tau\right] \\ & - 2C_- e^{-(\Gamma_{\rm qec}+6\Gamma_{\rm err}-6\frac{\Gamma_{\rm err}^2}{\Gamma_{\rm qec}})\tau}\cos\left[\omega\left(1+6\frac{\Gamma_{\rm err}}{\Gamma_{\rm qec}}\right)\tau\right], \end{aligned} \tag{7}$$

where $C_+ = \frac{1}{2} - \frac{3}{2}(\Gamma_{\rm err}/\Gamma_{\rm qec})$ and $C_- = -\frac{3}{2}(\Gamma_{\rm err}/\Gamma_{\rm qec})$. Simplifying further still, we arrive at

$$\langle \sigma_x^L \rangle \approx e^{-3\Gamma_{\rm eff}\,\tau}\cos[3\omega_{\rm eff}\tau] \tag{8}$$

[cf. (5)], where

$$\Gamma_{\rm eff} = 2\frac{\Gamma_{\rm err}}{\Gamma_{\rm qec}}\Gamma_{\rm err} \qquad \omega_{\rm eff} = \omega\left(1-2\frac{\Gamma_{\rm err}}{\Gamma_{\rm qec}}\right) \tag{9}$$

to first order in $\Gamma_{\rm qec}^{-1}$, as claimed above. In other words, imperfect QEC not only leads to logical decoherence; it also shifts the oscillation frequency of $\langle \sigma_x^L \rangle$. This is because the sensor acquires a relative phase at a rate 3ω in the absence of errors, but only at a rate ω in the brief intervals between an error and its subsequent correction. Therefore errors reduce the average precession rate $\omega_{\rm eff}$, and so $\omega_{\rm eff} < \omega$ for finite $\Gamma_{\rm qec}$. This bias is illustrated in the time and frequency domains in Figs. 1(b) and 1(c), respectively.

These figures show additionally that the bias is more pronounced in the error-corrected sensing situation than in an uncorrected one. This comes primarily from the fact that the leading-order behavior of the frequency scaling factor is in the latter case quadratic in the system's parameters [31] and not linear as shown in Eq. (9). The finite QEC rate will then act as an amplifier of the bias which in the non-corrected case was likely undetectable. While the fact that the transition from $\Gamma_{\rm qec} = 0$ to $\Gamma_{\rm qec} > 0$ does not fully eliminate the original bias is unsurprising, its transformation from a quadratic to a linear function in the dominant limits is an unexpected result.

Biasedness condition.—As mentioned previously, an alternative pragmatic representation of the qubits' evolution during the error-corrected sensing period is the repeated application of detection and correction processes $\mathcal{C}$ interspersed with sensing time intervals $\delta\tau$.

The evolution of the generic sensor can then be described by a set of three quantum channels: $\mathcal{N}, \mathcal{U}_{\delta\tau}$, and $\mathcal{C}$. The first element represents noise mechanisms which can be methodically approximated by a Pauli channel [50–52]. It is convenient to split it into noiseless and erroneous parts $\mathcal{N} = p_{\mathcal{I}}\mathcal{I} + p_{\mathcal{N}}\mathcal{N}'$, where $p_{\mathcal{I}} = 1 - p_{\mathcal{N}}$ is the probability that the state stays unharmed. $\mathcal{U}_{\delta\tau}(\rho) = U(\delta\tau)\rho U(\delta\tau)^\dagger$ with $U(\delta\tau) = \exp(-iH\delta\tau)$ expresses the unitary free evolution in the interval $\delta\tau$. The overall dynamics during the sensing time τ can then be approximated by the iteration of these three channels c times, such that $c\delta\tau = \tau$,

$$\begin{aligned} \rho \mapsto {} & \left[\prod_{k=1}^{c} \mathcal{C}\circ\mathcal{U}_{\delta\tau}\circ\mathcal{N}\right](\rho) \\ = {} & \left[p_{\mathcal{I}}\mathcal{C}\circ\mathcal{U}_{\delta\tau} + p_{\mathcal{N}}\mathcal{C}\circ\mathcal{U}_{\delta\tau}\circ\mathcal{N}'\right]^c(\rho). \end{aligned} \tag{10}$$

This expression can be simplified using the binomial theorem which is permitted here since in the logical subspace $\mathcal{C}\circ\mathcal{U}_{\delta\tau}$ commutes with $\mathcal{C}\circ\mathcal{U}_{\delta\tau}\circ\mathcal{N}'$ [31]. Finally, the discrete evolution can be reduced to the following form:

$$\rho \mapsto \sum_{k=0}^{c}\binom{c}{k} p_{\mathcal{I}}^{c-k} p_{\mathcal{N}}^{k}\left[\mathcal{C}\circ\mathcal{U}_{\delta\tau}\circ\mathcal{N}'\circ\mathcal{U}_{\delta\tau}^{-1}\right]^k(\rho_\tau), \tag{11}$$

with ρ_τ being the density matrix in the case of an ideal sensing protocol of duration τ, i.e., $\rho_\tau = \mathcal{U}_\tau(\rho) = \mathcal{U}_{\delta\tau}^c(\rho)$. Equation (11) reveals that finite rate QEC will systematically reduce the sensor's performance unless the erroneous subspaces evolve in the exact same manner as the logical one. In this scenario, $\mathcal{U}_{\delta\tau}\circ\mathcal{N}'$ and $\mathcal{U}_{\delta\tau}^{-1}$ would commute and reduce the expression to a unit channel. This is, for instance, the case in continuous-variable encodings where due to the continuity between the logical and error subspaces their evolutions do not differ. An example of electric field sensing using such encodings is discussed in the Supplemental Material [31]. The commutation relation $[\mathcal{U}_{\delta\tau}\circ\mathcal{N}', \mathcal{U}_{\delta\tau}^{-1}](\rho_L) = 0$ offers thus any experimenter a sanity check procedure for the biasedness of their error corrected sensing protocol.

Furthermore Eq. (11) represents an expected value of a CPTP map function $[\mathcal{C}\circ\mathcal{U}_{\delta\tau}\circ\mathcal{N}'\circ\mathcal{U}_{\delta\tau}^{-1}]^X$ with X being a

random variable following a binomial distribution. It can thus be approximated by a Taylor expansion around $\mathbb{E}[X] = cp_{\mathcal{N}}$,

$$\rho \rightsquigarrow \left[\mathcal{C} \circ \mathcal{U}_{\delta\tau} \circ \mathcal{N}' \circ \mathcal{U}_{\delta\tau}^{-1}\right]^{cp_{\mathcal{N}}} (\rho_\tau), \tag{12}$$

which is correct up to the second order in the expansion. This constitutes the biased evolution of the system without the exponential decoherence which appears from higher-order terms and central moments of $X \sim \mathrm{Bin}(c, p_{\mathcal{N}})$ [31]. In conclusion, to determine the amount of bias that a finite-rate QEC introduces in the outcome of a sensing protocol one must evaluate the expected value of the measured operator given in Eq. (12). In the Supplemental Material [31], we perform the analysis of our error-corrected Ramsey setting using this procedure and verify its agreement with simulations.

Biased parameter estimation.—Another method to assess the presence of a bias in a sensing protocol is to verify some statistical inequalities. A direct application of Eq. (5), i.e., equating ω with ω_{eff}, violates a fundamental bound of estimation theory known as Cramér-Rao lower bound [32]. On the contrary, the simple remedy in Eq. (9) almost completely resolves the issue, despite arising from a perturbative expansion. This result [31] obtained using Monte Carlo simulations of the presented system shows that the naïve estimator arising from Eq. (5) is biased. Perhaps more perniciously, we also show equating ω and ω_{eff} can give misleadingly optimistic figures of merit for error-corrected quantum sensors.

Minimum detectable signal.—A central figure of merit for a quantum sensor is the minimum detectable signal $|\delta\omega|$, defined as the smallest value of ω giving a unit signal to noise ratio [1]. Here $|\delta\omega| = 1/\sqrt{N\mathcal{I}(\omega)}$. The ideal case of $\langle\sigma_x^L\rangle = \cos(3\omega\tau)$ of perfect QEC, or noiseless qubits, gives a lower bound of $|\delta\omega|(\tau) \geq (9N\tau^2)^{-1/2}$ called the standard quantum limit (SQL).

A straightforward application of Eq. (5) would suggest a minimum detectable signal of

$$|\delta\omega|(\tau) \stackrel{?}{=} \sqrt{\frac{1 - e^{-6\Gamma_{\mathrm{err}}\tau}\cos^2[3\omega\tau]}{N9\,\tau^2\, e^{-6\Gamma_{\mathrm{err}}\tau}\sin^2[3\omega\tau]}}. \tag{13}$$

This expression equals the frequency uncertainty derived by Ref. [53]. It is minimized (smaller $|\delta\omega|$ is better) at the optimal sensing time

$$\tau_{\mathrm{opt}} = \frac{\pi}{2}\frac{k_{\mathrm{opt}}}{3\omega} \quad \text{with} \quad k_{\mathrm{opt}} = \left\lfloor \frac{2}{\pi}\frac{\omega}{\Gamma_{\mathrm{err}}} \right\rceil, \tag{14}$$

where $\lfloor\cdot\rceil$ indicates the rounding to the nearest integer. In contrast, the corresponding expression from Eq. (8) (i.e., accounting for $\omega \neq \omega_{\mathrm{eff}}$ and $\Gamma_{\mathrm{err}} \neq \Gamma_{\mathrm{eff}}$) is

$$|\delta\omega|(\tau) = \sqrt{\frac{1 - e^{-6\Gamma_{\mathrm{eff}}\tau}\cos^2[3\omega_{\mathrm{eff}}\tau]}{N9\tau^2(\partial_\omega\omega_{\mathrm{eff}})^2\, e^{-6\Gamma_{\mathrm{eff}}\tau}\sin^2[3\omega_{\mathrm{eff}}\tau]}}, \tag{15}$$

where $\partial_\omega\omega_{\mathrm{eff}}$ comes from the derivative of $\langle\sigma_x^L\rangle(\tau)$ with respect to ω. (The expression for $|\delta\omega|$ from the full Eq. (6) is lengthy and can be found in Ref. [31].) Since the former is equal to $1 - 2(\Gamma_{\mathrm{err}}/\Gamma_{\mathrm{qec}})$, independent of τ, the optimal sensing time is of the same form as in Eq. (14) but with the effective frequency and error rate substituted. In short, failing to account for the difference between $(\omega, \Gamma_{\mathrm{err}})$ and $(\omega_{\mathrm{eff}}, \Gamma_{\mathrm{eff}})$ would suggest an overly optimistic value of $|\delta\omega|$, off by a factor of $\sim|1 - 2(\Gamma_{\mathrm{err}}/\Gamma_{\mathrm{qec}})|$. We graphically illustrate this inconsistency as follows:

We consider a set of observations for which a frequency $\hat{\omega}$ and an error rate $\hat{\Gamma}_{\mathrm{err}}$ were estimated using the unadjusted expression in Eq. (5). Then, in the naïve scenario with $\hat{\omega} \equiv \omega$ and $\hat{\Gamma}_{\mathrm{err}} \equiv \Gamma_{\mathrm{err}}$, we insert them in Eq. (13) and calculate a first curve. In our proposed scenario, where we are aware of the existence of a bias, the estimated parameters stand for $\hat{\omega} \equiv \omega_{\mathrm{eff}}$ and $\hat{\Gamma}_{\mathrm{err}} \equiv \Gamma_{\mathrm{eff}}$. Substituting them into Eq. (15) yields a second curve. These two functions are presented in Fig. 2 as dashed and solid lines, respectively. Although both of them satisfy the standard quantum limit, only one can correctly reflect the true minimum detectable signal. We utilize the optimal sensing time to identify the correct function. To this end, we calculate τ_{opt} using Eq. (14) for both scenarios and plot the result in Fig. 2. As we can see, τ_{opt} comes out the same for both scenarios. This can be understood from the fact that it can either way be written as $\tau_{\mathrm{opt}} \approx (\hat{\Gamma}_{\mathrm{err}})^{-1}$. Yet, the computed τ_{opt} coincides with the minimum of the proposed function, while deviating from the naïve one. We thus conclude that only the proposed model delivers the true result for the minimum detectable signal.

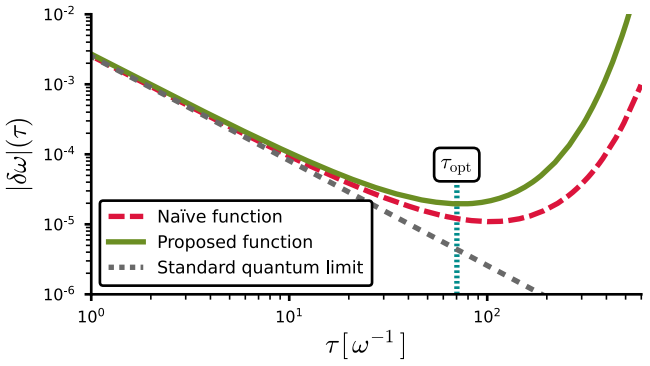

FIG. 2. Minimum detectable signal as a function of the sensing time τ for two different functions: naïve (dashed) and proposed (solid) using Eqs. (13) and (15), respectively. Both functions were plotted with the same values of $\hat{\omega}$ and $\hat{\Gamma}_{\mathrm{err}}$, for $\Gamma_{\mathrm{err}} = 0.2\omega$ and $\Gamma_{\mathrm{qec}} = 16.6\omega$. The optimal sensing time τ_{opt} calculated with Eq. (14) coincides with the minimum of the proposed function, thus establishing it as the correct model.

Discussion and conclusion.—In summary, we demonstrate in this work that quantum error correction of a finite frequency or strength in a quantum sensor not only introduces logical decoherence, but can also produce a systematic bias in the sensor's output. We showed that this effect can lead to overly optimistic—and even nonsensical—parameter estimates if unaccounted for, and proposed a remedy through postprocessing; an alternative method has been suggested in Ref. [54]. An interesting open question is whether it is possible to design QEC codes for sensing that do not introduce such a bias in the first place.

While we have focused on the bit-flip code for concreteness, we show that the phenomenon discussed here arises much more generally when the error operators do not commute with the sensor's Hamiltonian. Our results are not limited to Ramsey sensing schemes, even though we have focused on this approach. This work shows that nontrivial, and perhaps unexpected, effects can arise when performing QEC beyond the idealized limits considered in early proposals. We expect that much remains to be discovered in this direction on the way to realizing useful QEC.

I. R. thanks D. Roschewitz for helpful comments on the manuscript. This work was supported by the Swiss National Science Foundation (SNSF) through the National Centre of Competence in Research Quantum Science and Technology (NCCR QSIT) grant 51NF40–160591. I. R. and F. R. acknowledge financial support by the Swiss National Science Foundation (Ambizione Grant No. PZ00P2_186040).

*irojkov@ethz.ch
†Present address: IBM Quantum, Almaden Research Center, San Jose, California 95120, USA.
‡freiter@phys.ethz.ch

[1] C. L. Degen, F. Reinhard, and P. Cappellaro, Quantum sensing, Rev. Mod. Phys. **89**, 035002 (2017).
[2] L. Viola and S. Lloyd, Dynamical suppression of decoherence in two-state quantum systems, Phys. Rev. A **58**, 2733 (1998).
[3] J. M. Taylor, P. Cappellaro, L. Childress, L. Jiang, D. Budker, P. R. Hemmer, A. Yacoby, R. Walsworth, and M. D. Lukin, High-sensitivity diamond magnetometer with nanoscale resolution, Nat. Phys. **4**, 810 (2008).
[4] J.-M. Cai, B. Naydenov, R. Pfeiffer, L. P. McGuinness, K. D. Jahnke, F. Jelezko, M. B. Plenio, and A. Retzker, Robust dynamical decoupling with concatenated continuous driving, New J. Phys. **14**, 113023 (2012).
[5] J. E. Lang, R.-B. Liu, and T. S. Monteiro, Dynamical-Decoupling-Based Quantum Sensing: Floquet Spectroscopy, Phys. Rev. X **5**, 041016 (2015).
[6] A. Lazariev, S. Arroyo-Camejo, G. Rahane, V. K. Kavatamane, and G. Balasubramanian, Dynamical sensitivity control of a single-spin quantum sensor, Sci. Rep. **7**, 6586 (2017).
[7] S. Schmitt, T. Gefen, F. M. Stürner, T. Unden, G. Wolff, C. Müller, J. Scheuer, B. Naydenov, M. Markham, S. Pezzagna, J. Meijer, I. Schwarz, M. B. Plenio, A. Retzker, L. P. McGuinness, and F. Jelezko, Submillihertz magnetic spectroscopy performed with a nanoscale quantum sensor, Science **356**, 832 (2017).
[8] G. T. Genov, N. Aharon, F. Jelezko, and A. Retzker, Mixed dynamical decoupling, Quantum Sci. Technol. **4**, 035010 (2019).
[9] M. Ban, Photon-echo technique for reducing the decoherence of a quantum bit, J. Mod. Opt. **45**, 2315 (1998).
[10] R. Ozeri, Heisenberg limited metrology using quantum error-correction codes, arXiv:1310.3432.
[11] E. M. Kessler, I. Lovchinsky, A. O. Sushkov, and M. D. Lukin, Quantum Error Correction for Metrology, Phys. Rev. Lett. **112**, 150802 (2014).
[12] W. Dür, M. Skotiniotis, F. Fröwis, and B. Kraus, Improved Quantum Metrology Using Quantum Error Correction, Phys. Rev. Lett. **112**, 080801 (2014).
[13] G. Arrad, Y. Vinkler, D. Aharonov, and A. Retzker, Increasing Sensing Resolution with Error Correction, Phys. Rev. Lett. **112**, 150801 (2014).
[14] D. A. Herrera-Martí, T. Gefen, D. Aharonov, N. Katz, and A. Retzker, Quantum Error-Correction-Enhanced Magnetometer Overcoming the Limit Imposed by Relaxation, Phys. Rev. Lett. **115**, 200501 (2015).
[15] M. B. Plenio and S. F. Huelga, Sensing in the presence of an observed environment, Phys. Rev. A **93**, 032123 (2016).
[16] T. Gefen, D. A. Herrera-Martí, and A. Retzker, Parameter estimation with efficient photodetectors, Phys. Rev. A **93**, 032133 (2016).
[17] F. Reiter, A. S. Sørensen, P. Zoller, and C. A. Muschik, Dissipative quantum error correction and application to quantum sensing with trapped ions, Nat. Commun. **8**, 1822 (2017).
[18] Y. Matsuzaki and S. Benjamin, Magnetic-field sensing with quantum error detection under the effect of energy relaxation, Phys. Rev. A **95**, 032303 (2017).
[19] T. Unden, P. Balasubramanian, D. Louzon, Y. Vinkler, M. B. Plenio, M. Markham, D. Twitchen, A. Stacey, I. Lovchinsky, A. O. Sushkov, M. D. Lukin, A. Retzker, B. Naydenov, L. P. McGuinness, and F. Jelezko, Quantum Metrology Enhanced by Repetitive Quantum Error Correction, Phys. Rev. Lett. **116**, 230502 (2016).
[20] L. Cohen, Y. Pilnyak, D. Istrati, A. Retzker, and H. S. Eisenberg, Demonstration of a quantum error correction for enhanced sensitivity of photonic measurements, Phys. Rev. A **94**, 012324 (2016).
[21] M. Bergmann and P. van Loock, Quantum error correction against photon loss using noon states, Phys. Rev. A **94**, 012311 (2016).
[22] P. Sekatski, M. Skotiniotis, J. Kołodyński, and W. Dür, Quantum metrology with full and fast quantum control, Quantum **1**, 27 (2017).
[23] S. Zhou, M. Zhang, J. Preskill, and L. Jiang, Achieving the heisenberg limit in quantum metrology using quantum error correction, Nat. Commun. **9**, 78 (2018).
[24] R. Demkowicz-Dobrzański, J. Czajkowski, and P. Sekatski, Adaptive Quantum Metrology under General Markovian Noise, Phys. Rev. X **7**, 041009 (2017).

[25] D. Layden and P. Cappellaro, Spatial noise filtering through error correction for quantum sensing, Quantum Inf. **4**, 30 (2018).
[26] D. Layden, S. Zhou, P. Cappellaro, and L. Jiang, Ancilla-Free Quantum Error Correction Codes for Quantum Metrology, Phys. Rev. Lett. **122**, 040502 (2019).
[27] W. Górecki, S. Zhou, L. Jiang, and R. Demkowicz-Dobrzański, Optimal probes and error-correction schemes in multi-parameter quantum metrology, Quantum **4**, 288 (2020).
[28] D. A. Lidar and T. A. Brun, *Quantum Error Correction* (Cambridge University Press, Cambridge, England, 2013).
[29] Instead of considering $H \propto \sigma_z$ and $L_{\mathrm{err}} \propto \sigma_x$, some works looked at the problem from the opposite point of view by taking $H \propto \sigma_x$ and $L_{\mathrm{err}} \propto \sigma_z$. This only changes the codewords used by the sensing protocol but not the conclusions of our work since the signal and the noise remain perpendicular in both cases.
[30] N. F. Ramsey, A molecular beam resonance method with separated oscillating fields, Phys. Rev. **78**, 695 (1950).
[31] See Supplemental Material at http://link.aps.org/supplemental/10.1103/PhysRevLett.128.140503, which includes Refs. [32–49].
[32] H. Cramér, *Mathematical Methods of Statistics (PMS-9)* (Princeton University Press, Princeton, NJ, 1999).
[33] A. C. Berry, The accuracy of the Gaussian approximation to the sum of independent variates, Trans. Am. Math. Soc. **49**, 122 (1941), publisher: American Mathematical Society.
[34] C. G. Esseen, On the Liapunov limit error in the theory of probability, Ark. Mat. Astron. Fys. **28**, 1 (1942).
[35] C. Flühmann, V. Negnevitsky, M. Marinelli, and J. P. Home, Sequential Modular Position and Momentum Measurements of a Trapped Ion Mechanical Oscillator, Phys. Rev. X **8**, 021001 (2018).
[36] C. Flühmann, Encoding a qubit in the motion of a trapped ion using superpositions of displaced squeezed states, Doctoral thesis, ETH Zurich, 2019.
[37] C. Flühmann, T. L. Nguyen, M. Marinelli, V. Negnevitsky, K. Mehta, and J. P. Home, Encoding a qubit in a trapped-ion mechanical oscillator, Nature (London) **566**, 513 (2019).
[38] P. Campagne-Ibarcq, A. Eickbusch, S. Touzard, E. Zalys-Geller, N. E. Frattini, V. V. Sivak, P. Reinhold, S. Puri, S. Shankar, R. J. Schoelkopf, L. Frunzio, M. Mirrahimi, and M. H. Devoret, Quantum error correction of a qubit encoded in grid states of an oscillator, Nature (London) **584**, 368 (2020).
[39] B. de Neeve, T. L. Nguyen, T. Behrle, and J. Home, Error correction of a logical grid state qubit by dissipative pumping, Nat. Phys. 1 (2022).
[40] R. Maiwald, D. Leibfried, J. Britton, J. C. Bergquist, G. Leuchs, and D. J. Wineland, Stylus ion trap for enhanced access and sensing, Nat. Phys. **5**, 551 (2009).
[41] W. C. Campbell and P. Hamilton, Rotation sensing with trapped ions, J. Phys. B **50**, 064002 (2017).
[42] M. J. Biercuk, H. Uys, J. W. Britton, A. P. VanDevender, and J. J. Bollinger, Ultrasensitive detection of force and displacement using trapped ions, Nat. Nanotechnol. **5**, 646 (2010).
[43] R. Shaniv and R. Ozeri, Quantum lock-in force sensing using optical clock Doppler velocimetry, Nat. Commun. **8**, 14157 (2017).
[44] K. Duivenvoorden, B. M. Terhal, and D. Weigand, Single-mode displacement sensor, Phys. Rev. A **95**, 012305 (2017).
[45] F. Wolf, C. Shi, J. C. Heip, M. Gessner, L. Pezzè, A. Smerzi, M. Schulte, K. Hammerer, and P. O. Schmidt, Motional Fock states for quantum-enhanced amplitude and phase measurements with trapped ions, Nat. Commun. **10**, 2929 (2019).
[46] D. Gottesman, A. Kitaev, and J. Preskill, Encoding a qubit in an oscillator, Phys. Rev. A **64**, 012310 (2001).
[47] J. Liu, H. Yuan, X.-M. Lu, and X. Wang, Quantum Fisher information matrix and multiparameter estimation, J. Phys. A **53**, 023001 (2020).
[48] S. Geman, E. Bienenstock, and R. Doursat, Neural networks and the bias/variance dilemma, Neural Comput. **4**, 1 (1992).
[49] J. R. Johansson, P. D. Nation, and F. Nori, QuTiP2: A PYTHON framework for the dynamics of open quantum systems, Comput. Phys. Commun. **184**, 1234 (2013).
[50] J. J. Wallman and J. Emerson, Noise tailoring for scalable quantum computation via randomized compiling, Phys. Rev. A **94**, 052325 (2016).
[51] R. Harper, S. T. Flammia, and J. J. Wallman, Efficient learning of quantum noise, Nat. Phys. **16**, 1184 (2020).
[52] M. Ware, G. Ribeill, D. Ristè, C. A. Ryan, B. Johnson, and M. P. da Silva, Experimental Pauli-frame randomization on a superconducting qubit, Phys. Rev. A **103**, 042604 (2021).
[53] S. F. Huelga, C. Macchiavello, T. Pellizzari, A. K. Ekert, M. B. Plenio, and J. I. Cirac, Improvement of Frequency Standards with Quantum Entanglement, Phys. Rev. Lett. **79**, 3865 (1997).
[54] K. Yamamoto, S. Endo, H. Hakoshima, Y. Matsuzaki, and Y. Tokunaga, Error-mitigated quantum metrology, arXiv:2112.01850.